



Full Length Research Paper

Properties of (Cd, Zn)S films deposited by DC co-sputtering

Lwitiko P. Mwakyusa

Department of Physics, Solar Energy, and Materials Science Group, University of Dar es Salaam
(UDSM), P.O. Box 35063, Dar es Salaam, Tanzania

E-mail: mwakyusa.lwitiko@udsm.ac.tz ORCID: <https://orcid.org/0000-0001-6691-695X>

ABSTRACT

CdS thin film is commonly used as a buffer layer in most thin film solar cells. However, the buffer layer with less absorption in the visible region of the solar spectrum as well as that which provides perfect lattice matching with the absorbers is required. The incorporation of Zn in the CdS films can affect the structural and optical properties of the buffer layer. In this work, films of CdS and (Cd,Zn)S films were deposited by DC sputtering utilizing CdS and Zn targets. The concentration of Zn in the CdS was varied by changing the sputtering power of the Zn target. The influence of Zn concentration on the structural and optical properties of CdS films was investigated using X-ray diffraction (XRD) and Ultraviolet-Visible-Near Infrared (UV-VIS-NIR) spectroscopy, respectively. The XRD patterns confirm the growth preferential orientation of all films along the (002) plane. UV-VIS spectroscopy results indicate absorption edge shifts toward lower wavelength with an increase of Zn concentration in the CdS. The band gap evaluated by the Tauc plot of these films varied from 2.40 eV to 2.50 eV ($0 \leq x \leq 0.14$). The increased bandgap induces the density of localized states on the edge of the bandgap which leads to the increase in the Urbach tail width.

ARTICLE INFO

Submitted: September 22, 2022

Revised: November 18, 2022

Accepted: December 8, 2022

Published: December 30, 2022

Keywords: CdS thin film, Buffer layer, (Cd, Zn)S thin film, Co-sputtering

INTRODUCTION

II-VI semiconductor thin films have attracted considerable attention from the photovoltaic (PV) community as they can be used as a buffer layer in thin-film solar cells (Ikhmayies and Ahmad-Bitar, 2013; Mwakyusa *et al.*, 2019). For instance, CdS film is commonly used as a buffer layer in Cu(In,Ga)Se₂ (CIGS) solar cells. Using this type of buffer layer devices with efficiencies up to 23.2% could be realized (Mwakyusa *et al.*, 2022). CdS thin film is characterized by a wide bandgap (2.40 eV) (Mahdi and Al-Ani, 2012; Bakly *et al.*, 2018; Settu *et al.*,

2019). Considering this bandgap, CdS films are expected to absorb photons with a wavelength lower than 590 nm—which covers about 24% of the solar spectrum (Devadoss *et al.*, 2014; Jhuma *et al.*, 2019). This is expected to lower the short-circuit current density (J_{sc}) of thin film solar cells, hence the overall conversion efficiency. Bandgap engineering of CdS is a promising approach to avoiding this problem. Experimentally, this could be easily realized through doping. It is well known that semiconductor doping has the potential of

modulating the structural, optical, and electrical properties of the materials. For instance, it has been demonstrated that the bandgap of CdS films can be tuned from 2.35 eV to 2.50 eV by doping with an appropriate amount of In (Ikhmayies and Ahmad-Bitar, 2013). About *et al.*, (2019) reported a decrease in the CdS bandgap when Cu atoms were used as dopants. Moreover, it has been documented that the bandgap of CdS films can be controlled by combining CdS (2.4 eV) and Zn (3.7 eV) (Mahdi and Al-Ani, 2012; Bakly *et al.*, 2018). Following this approach, the ternary phase of (Cd,Zn)S with a bandgap in the range between 2.4 eV to 3.7 eV could be demonstrated (Mahdi and Al-Ani, 2012). It was experimentally demonstrated that the bandgap of CdS can be controlled in the range of 2.40 eV (undoped) to 3.65 eV (doped) by adjusting the amount of Zn (Pawar *et al.*, 2011). A similar observation has been reported by (Mahdi and Al-Ani, 2012). Song *et al.*, (2006) showed that the bandgap of CdS films can be tuned from 2.40 eV to 2.7 eV by incorporating about 30% of Zn in the bath solution. The bandgap of up to 3.16 eV of (Cd,Zn)S films has been reported by (Patidar *et al.*, 2008). Following this line of argument, it is clear that it is possible to tune the bandgap of CdS film by incorporating Zn. It could be concluded that Zn incorporation into the CdS lattice is expected to boost the conversion efficiency of thin film solar cells. Commonly, CdS and (Cd,Zn)S films are prepared by chemical bath deposition (CBD) (Kostoglou *et al.*, 2001; Li *et al.*, 2005; Chadel *et al.*, 2015; Mwakyusa *et al.*, 2019; Settu *et al.*, 2019). This approach is relatively simple and cheap. However, the CBD process produces a larger amount of Cd waste. Moreover, to obtain films with high quality, the value of pH must be maintained at around 7.0 (Song *et al.*, 2005). Further, it is known that CdS is less soluble ($k_{sp} \sim 10^{-28}$) than ZnS ($k_{sp} \sim 10^{-23.8}$), thus the formation of (Cd,Zn)S films becomes more difficult (Mahdi and Al-Ani, 2012). To avoid this problem, in this work CdS and

(Cd,Zn)S films have been prepared by DC sputtering utilizing CdS and Zn targets. To investigate the effect of the amount of Zn in the CdS lattice, the sputtering power of the Zn target varied from 0–10 W in the interval of 5 W. Low sputtering power was utilized to avoid the formation of metallic Zn in the films. The influence of Zn amount in the CdS properties was examined and discussed.

MATERIAL AND METHODS

Sample preparation

CdS and (Cd,Zn)S films were deposited onto soda-lime glass (SLG) and 500 nm molybdenum-coated soda lime glass (Mo/SLG) substrates via a co-sputtering using BALZERS BAE 250 coating unit. For CdS films, a ceramic target (99.99% supplied by Plasmaterials Inc.) was used while for (Cd,Zn) films, CdS and Zn (99.99% supplied by Plasmaterials Inc.) were co-sputtered onto SLG. Prior to deposition, the SLG was cleaned as ascribed by (Mwakyusa *et al.*, 2022). After ultrasonically cleaning the substrate, the substrates were loaded into the sputtering chamber then the unit was evacuated to a base pressure of around 10^{-6} mbar. During the deposition, the Ar gas flow rate and working pressure were fixed to 30 sccm and 6.4×10^{-3} mbar, respectively. Both films were deposited at a temperature of approximately 100 °C. For CdS, the sputtering power was fixed at 60 W while that of Zn was varied from 0-10 W with the motivation of investigating the effect of Zn incorporation on the optical properties of CdS films. All samples were deposited for 20 mins with a view of obtaining a film with a thickness of around 100 nm. Three samples labeled CdS_ref, (Cd,Zn)S_Zn(5W), and (Cd,Zn)S_Zn(10W) were prepared and analyzed.

Characterization

To analyze film thicknesses, the Alpha step IQ profilometer was used. The films crystallinity and phase identification studies

were carried out using an X-ray diffractometry (XRD, Bruker, D2 phase) diffractometer system with a Cu-K α 1 ($\lambda = 1.540629\text{\AA}$) radiation operated at 40 mA and 40 kV with Bragg-Brentano θ - 2θ scanning mode. The samples were scanned from 10° to 80° at room temperature. The material phases were analyzed as ascribed by (Mwakyusa *et al.*, 2022). Using a Gauss fit, the value of Full Width at Half Maximum (FWMH) of the dominant XRD peak was evaluated. The crystallite size of all samples was evaluated as described in (Mwakyusa *et al.*, 2022). Optical transmittance was measured by using a UV-VIS-NIR double beam spectrophotometer equipped with an integrated sphere (Perkin Elmer Lambda 19) in the wavelength range $300\text{ nm} \leq \lambda \leq 2000\text{ nm}$ at room temperature.

RESULTS AND DISCUSSION

It is well known that CdS films can be crystallized into two forms: i) the hexagonal (wurtzite) phase and ii) the cubic (zincblende) phase. To end this, the main material phases of the sputtered CdS and (Cd,Zn)S were analyzed by XRD measurements. The XRD spectra for both CdS and (Cd,Zn)S are displayed in Figure 1(a) with a detailed view of the dominant peak (002) in Figure 1(b). All the XRD peaks are assigned according to ICCD No.: 00-041-1049. It is worth noting that the XRD peak position (002) has been corrected using (110) dominant peak of Mo which appears at 40.5. As can be seen, the films are composed of (002) and (202) peaks. The absence of XRD peaks at 30.6 reveals that these patterns correspond to the polycrystalline hexagonal phase and are orientated with the *c*-axis perpendicular to the substrate. This preferred orientation observed is due to the controlled nucleations of adatoms associated with the relatively low deposition rate of CdS and

(Cd,Zn)S films (Li *et al.*, 2006). This suggests that there is preferential columnar growth parallel to the substrate—meaning that there are no grain boundaries parallel to the junction which could prevent the flow of photocurrent generated (Li *et al.*, 2006). No phases related to metallic Zn or ZnS were observed. It strongly indicates that Zn is incorporated into the CdS lattice. Interestingly, we notice that the XRD peaks (002) are shifted to higher Bragg angles with increasing sputtering power in Zn targets (see Figure 1 (b)). The sequential shifts of the dominant XRD peaks suggest that Zn atoms are incorporated in the CdS lattice to form (Cd,Zn)S films. These findings are in good agreement with previous reports (Patidar *et al.*, 2008; Bakly *et al.*, 2018). Using a Gauss fit, the value of the Full Width at Half Maximum (FWHM) values of the dominant peak were extracted. From Table 1, it can be seen that the FWHM decreased with an increase in the amounts of Zn. It is an indication of the improvement of the crystallinity of the CdS films with the addition of Zn (Li *et al.*, 2006; Mwakyusa *et al.*, 2022). The improvement of crystallinity can be associated with the increase in grain size. To address this aspect, the values of crystallite size for all samples were evaluated. The calculated values of crystallite size are presented in Table 1. The crystallite size increased with an increase in Zn amounts in the CdS lattice. The calculated crystallite values are somewhat comparable with those reported by the CBD approach (Settu *et al.*, 2019). This is attributed to a slow deposition rate (around 5 nm/min). A slow deposition rate allows the adatoms to have the space to develop to the larger crystallite size and consequently to the larger grains. The increase in the crystallite size is an indication that the films are becoming more compact and the transmittance efficiency is expected to be improved (Heiba *et al.*, 2015).

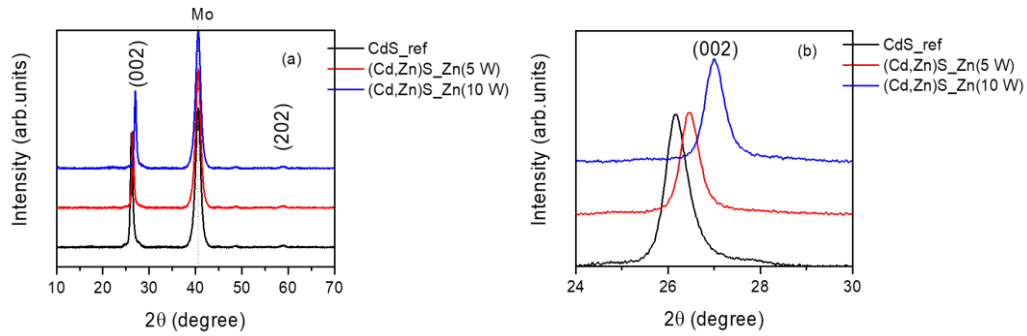


Figure 1: (a) XRD scans, (b) detailed view of the (002) XRD peak for CdS with different concentrations of Zn.

Table 1: (002) XRD peak positions, extracted FWHM, and calculated crystallite size for CdS with different concentrations of Zn.

Sample	2θ (degree)	FWHM (degree)	Crystallite size (nm)
CdS_ref	26.64	0.61	29.80
(Cd,Zn)S_Zn(5W)	26.94	0.50	35.90
(Cd,Zn)S_Zn(10W)	27.46	0.51	34.50

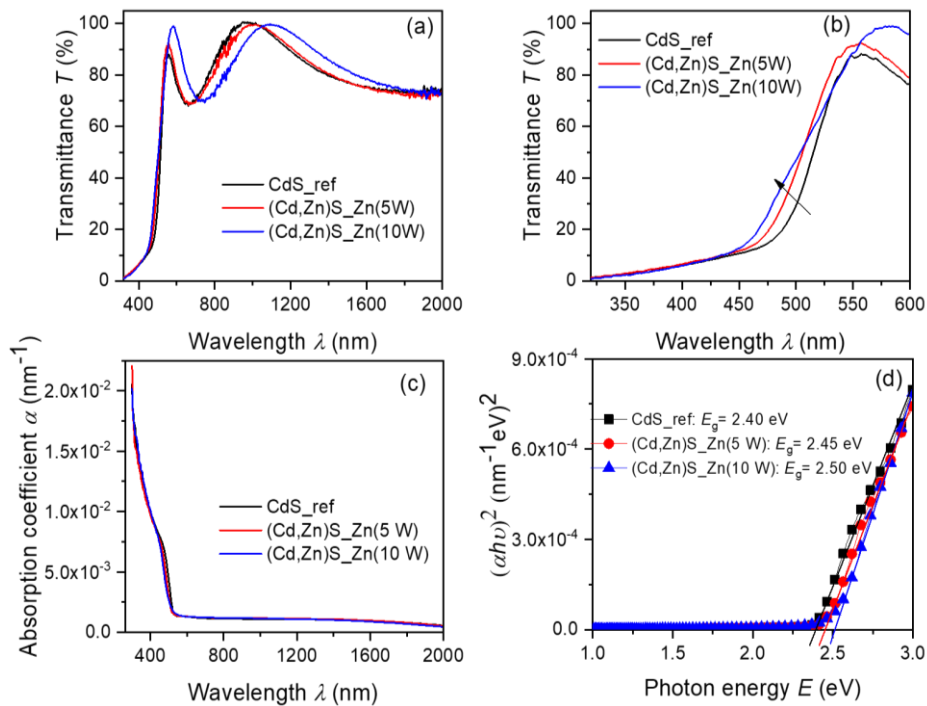


Figure 2: (a) the transmittance spectra, (b) a detailed view of transmittance spectra at lower wavelength, (c) dependence of absorption coefficient on the wavelength, and (d), the $(\alpha h\nu)^2$ versus photon energy curves for CdS with different amounts of Zn.

It is well known that high optical transparency is an important factor for *n*-type compound semiconductors to be used as a buffer layer in thin-film solar cells. The optical properties of the CdS and (Cd,Zn)S were investigated by observing the UV-VIS-

NIR transmittance properties. The optical transmission spectra of the CdS with different amounts of Zn are shown in Figure 2 (a). As can be seen, all the films were highly transparent in the visible and NIR regions. A very sharp absorption edge in the

UV region is visible in all samples. This suggests that films are somewhat free from defects in the band edges and hence less Urbach tail effect. As it appeared in Figure 2(b), a shift of the absorption tail toward a shorter wavelength with increasing in the amount of Zn in CdS films. This finding is in good agreement with previous reports (Mahdi and Al-Ani, 2012; Bakly *et al.*, 2018). It is important to note that Urbach energy (E_u) is the optical quantity that could be to quantify the grade of structural disturbance in thin films. To address this aspect, the values of E_u were calculated as documented by (Mahdi and Al-Ani, 2012). Figure 3 shows the dependence $\ln\alpha$ on photon energy, with a linear fit yielding the slope which can be used to calculate the value of E_u . As shown in Figure 3, the value of E_u increases with an increase in the amount of Zn but not linearly. However, our values are in good agreement with those reported by (Ikhmayies and Ahmad-Bitar,

2013; Hasaneen *et al.*, 2020). These results and findings from the previous reports suggest that Zn incorporation somewhat induces the density of localized states on the edge of the bandgap (Ikhmayies and Ahmad-Bitar, 2013). As documented by Hasaneen *et al.*, (2020) that the Urbach tail decreases directly with an increase in the optical energy band gap. Based on these findings it could be hypothesized that Zn incorporation may not significantly impact the optical bandgap of CdS film. As a proof of concept, the values of the bandgap of undoped and doped samples were estimated as described by (Mwakyusa *et al.*, 2022). It was found that the bandgap increases from 2.40 eV for undoped to 2.50 eV for doped CdS (see Figure 2(d)). As expected the bandgap showed no linear relationship with E_u . These results further support our argument for the increase of the E_u with Zn amount as described before.

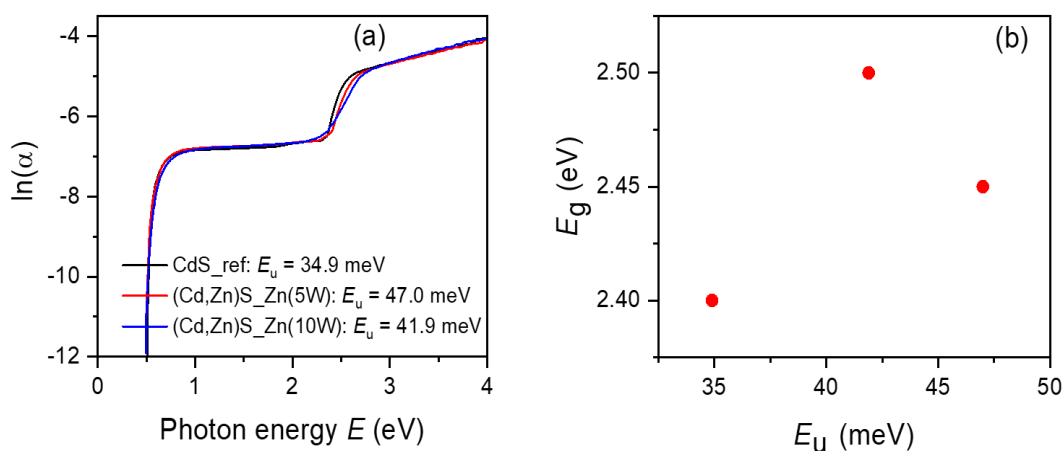


Figure 3: (a) the plot of $\ln(\alpha)$ and vs the photon energy and (b) the relationship between the bandgap energy and the width of the Urbach tail for CdS with different amounts of Zn.

Table 2: Average $[Zn]/[Zn] + [Cd]$ ratios for (Cd,Zn)S films prepared with different amounts of Zn.

Sample	CdS_ref	(Cd,Zn)S_Zn(5W)	(Cd,Zn)S_Zn(10W)
$[Zn]/[Zn] + [Cd]$	0	0.01	0.14

Using the extracted bandgap values, the average ratio of the $[Zn]/[Zn] + [Cd]$ in the films was estimated from Vegard's

expression as described by (Mahdi and Al-Ani, 2012).

$$E_g = E_g(0) + 0.69x + 0.62x^2 \quad (1)$$

where, $E_g(0)$ is the bandgap of pure CdS which is 2.40 eV. As expected the average ratio of the $[Zn]/[Zn] + [Cd]$ increases with increasing in sputtering power to the Zn target (see Table 2). These results are in good agreement with peak shifting observed in the XRD patterns. Based on these

findings it could be concluded that co-sputtering of CdS and Zn targets is a feasible approach for preparing (Cd,Zn)S buffer layer for thin film solar cells without producing a significant amount of CdS waste.

CONCLUSION

In summary, CdS and (Cd,Zn)S films were deposited by DC sputtering. The concentration of Zn in the films was varied by changing the sputtering power in the Zn target. The X-ray diffraction analysis revealed that these films were hexagonal polycrystalline with (002) a preferred orientation perpendicular to the glass substrate. UV-VIS spectroscopy showed that the extracted bandgap increased from 2.40 eV to 2.50 eV as sputtering power in the Zn target increased from 0 – 10 W. The calculated average ratio of $[Zn]/[Zn] + [Cd]$ increases with increasing in sputtering power to the Zn target. This deposition approach could be potential for deposition of (Cd,Zn)S buffer layer in CIGS and kesterite-based solar cells.

ACKNOWLEDGMENT

The author gratefully acknowledges the International Science Program (ISP) of Uppsala University, Sweden, and the Materials Science and Solar Energy Network for Eastern and Southern Africa (MSSEESA) for research materials and facilities. Further, the author thanks Dr. Ngei Kitumo at KIT for the XRD measurements.

REFERENCES

About A. A., Mukherjee A., Revaprasadu N. and Mohamed A.N. (2019). The effect of Cu-doping on CdS thin films deposited by the spray pyrolysis technique. *J. Mater. Res. Technol.* **8** (2): 2021–2030.

Bakly A.A.K., Spencer B.F., and O'Brien P. (2018). The deposition of thin films of cadmium zinc sulfide $Cd_{1-x}Zn_xS$ at 250 °C from spin-coated xanthato complexes: a potential route to window layers for photovoltaic cells. *J. Mater. Sci.* **53** (6):

4360–4370.

Chadel A., Benyoucef B. and Chadel M. (2015). A comparative study of CIGS solar cells based on Zn (O, S) buffer layers and CIGS solar cells based on CdS buffer layers. *Optoelectron. Adv. Mater. Rapid Commun.* **9** (5–6): 653–656.

Devadoss I., Muthukumar S. and Ashokkumar M. (2014). Structural and optical properties of $Cd_{1-x}Zn_xS$ ($0 \leq x \leq 0.3$) nanoparticles. *J. Mater. Sci. Mater. Electron.* **25** (8): 3308–3317.

Hasaneen M.F., Taya Y.A., Ali H.M., and Ahmed M.R. (2020). Optical and structure properties of CdTe/CdS films under influence of both CdCl₂ heat treatment and (O₂ + Ar) atmosphere. *Appl. Phys. A Mater. Sci. Process.* **126** (7): 1–12.

Heiba Z.K., Imam N. G., and Mohamed M.B., (2015). Coexistence of cubic and hexagonal phases of Cd doped ZnS at different annealing temperatures. *Mater. Sci. Semicond. Process.* **34**: 39–44.

Ikhmayies S. J., and Ahmad-Bitar R.N., (2013). A study of the optical bandgap energy and Urbach tail of spray-deposited CdS:In thin films. *J. Mater. Res. Technol.* **2**(3): 221–227.

Jhuma F.A., Shaily M.Z., and Rashid M.J. (2019). Towards high-efficiency CZTS solar cell through buffer layer optimization. *Mater. Renew. Sustain. Energy* **8** (1): 1–7.

Kostoglou M., Andritsos N., and Karabelas A.J. (2001). Progress towards modeling the CdS chemical bath deposition process. *Thin Solid Films* **387** (1–2): 115–117.

Li W., Cai X., Chen Q. and Zhou Z. (2005). Influence of growth process on the structural, optical, and electrical properties of CBD-CdS films. *Mater. Lett.* **59** (1): 1–5.

Li X., Li W., and Dong X. (2006). Effects of growth process on structural and optical properties of chemical bath deposition cadmium sulfide thin films. *Japanese J. Appl. Physics, Part 1 Regul. Pap. Short Notes Rev. Pap.* **45** (12): 9108–9110.

Mahdi M.A. and Al-Ani S.K.J. (2012). Optical characterization of chemical bath deposition $Cd_{1-x}Zn_xS$ thin films. *Int. J. Nanoelectron. Mater.* **5** (1): 11–24.

Mwakyusa L.P., Mlyuka N.R. and Samiji M.E. (2022). Boron Doped ZnO Films Deposited by DC Reactive Sputtering

- Using Zn:B Target: Influence of the Deposition Temperature on the Structural, Electrical and Optical Properties. *Tanzania J. Sci.* **48**(1): 148–155.
- Mwakyusa L.P., Neuwirth M., Kogler W., Schnabel T., Ahlswede E., Paetzold U.W., Richards B.S. and Hetterich M. (2019). CZTSe solar cells prepared by co-evaporation of multilayer Cu–Sn/Cu,Zn,Sn,Se/ZnSe/Cu,Zn,Sn,Se stacks. *Phys. Scr.* 94 (10): 105007.
- Patidar D., Saxena N.S., and Sharma T.P. (2008) Structural, optical and electrical properties of CdZnS thin films. *J. Mod. Opt.* **55** (1): 79–88.
- Pawar S.M., Pawar B.S., Kim J.H., Joo O.S. and Lokhande C.D. (2011). Recent status of chemical bath deposited metal chalcogenide and metal oxide thin films. *Curr. Appl. Phys.* **11**(2): 117–161.
- Settu P., Gobi G., Baskaran P. and Manikandan K. (2019) Effect of Zinc concentration in CdS thin films deposited in complexing agent by chemical bath deposition: Structural, optical, morphological and topographical studies. *Mater. Res. Express* **6** (12):
- Song J., Li S.S., Yoon S., Kim W.K., Kim J., Chen J., Craciun V., Anderson T.J., Crisalle O.D. and Ren F. (2005) Growth and characterization of CdZnS thin film buffer layers by chemical bath deposition. *Conf. Rec. IEEE Photovolt. Spec. Conf.:* 449–452.